Composites: Part A 54 (2013) 1–9

Contents lists available at SciVerse ScienceDirect

Composites: Part A

journal homepage: www.elsevier.com/locate/compositesa

Facile synthesis of lanthanum hypophosphite and its application in glass-fiber reinforced polyamide 6 as a novel flame retardant ☆

Gang Tang [a,b], Xin Wang [a], Rui Zhang [c], Wei Yang [a,b], Yuan Hu [a,b,*], Lei Song [a], Xinglong Gong [a,d,*]

[a] State Key Laboratory of Fire Science, University of Science and Technology of China, 96 Jinzhai Road, Hefei, Anhui 230026, PR China
[b] Suzhou Key Laboratory of Urban Public Safety, Suzhou Institute for Advanced Study, University of Science and Technology of China, 166 Ren'ai Road, Suzhou, Jiangsu 215123, PR China
[c] College of Chemical Engineering, Nanjing Forestry University, 159 Longpan Road, Nanjing, Jiangsu 210037, PR China
[d] CAS Key Laboratory of Mechanical Behavior and Design of Materials, Department of Modern Mechanics, University of Science and Technology of China, Hefei, Anhui 230026, PR China

ARTICLE INFO

Article history:
Received 25 January 2013
Received in revised form 29 May 2013
Accepted 2 July 2013
Available online 11 July 2013

Keywords:
A. Glass fibers
A. Polymer–matrix composites (PMCs)
A. Particle-reinforcement
B. Mechanical properties

ABSTRACT

This work developed flame retarded glass fiber reinforced polyamide 6 (FR-GFPA) composites with excellent mechanical properties, thermal stability and flame retardancy using a novel flame retardant, lanthanum hypophosphite (LaHP). The flame-retarded properties of FR-GFPA composites were characterized by limiting oxygen index, Underwriters Laboratories 94 testing and cone calorimeter test. FR-GFPA composite with 20 wt% LaHP reached V-0 rating and a high LOI value (27.5 vol%). The mechanical performance analysis showed that both the storage modulus and tensile strength increased and then decreased with the increase of LaHP loading. For FR-GFPA composite with 15 wt% LaHP loading, the storage modulus was 164% higher than that of glass fiber reinforced polyamide 6 (GFPA). Thermogravimetric analysis (TGA) and char residue characterization showed that the addition of LaHP can promote the formation of compact physical char barrier, reduce the mass loss rate and thus improve the flame retardancy of FR-GFPA composites.

1. Introduction

Glass-fiber reinforced polyamide 6 (GRPA) is an attractive engineering material which is widely used in electronic or electrical equipment, military and civil infrastructure applications due to its excellent mechanical properties, heat resistance and oil resistance [1,2]. However, like to most polymers, polyamide 6 shows poor fire resistance due to its petroleum origin. Furthermore, the presence of glass fiber enhance the flammability of polyamide 6 matrix because of "wick effect" for the propagation of the combustion by increasing effectiveness of heat transform in the burning area [3]. Thus, the research of flame retarded GRPA composites is a major concern for academic institutions and industrial laboratories. And also, the applications of polyamide in electrical industry promote the research of flame retardancy of polyamide composites [4].

In the past decades, the flame retardant containing halogen additives were mostly used for glass fiber reinforced polymer composites. However, some of the halogen-containing flame retardant have been forbidden to use in the world wide for releasing toxic and corrosive gas in burning process. Thus, the development of halogen-free flame retardant is the trend in the field of flame retarded composites.

Traditional phosphorus and nitrogen-based flame retardant, such as ammonium polyphosphate (APP), melamine cyanurate (MCA), and melamine polyphosphate (MPP) have been successfully applied in those composites [5–8]. Levchik et al. used APP as flame retardants for polyamide 6, in which PA6/APP composites presented high LOI value when APP loading was 40–50 wt% [5]. Chen and Wang focused on the in situ preparation of melamine cyanurate (MCA) nanoparticles from the reaction of melamine and cyanuric acid, and the flame retarded polyamide 6 composite in the extrusion process by a novel processing method provided a new strategy for flame retardancy of polyamide [6]. Tai et al. investigated flame-retarded glass fiber reinforced polyamide 6 composites using melamine polyphosphate (MPP), and found that organically modified iron-montmorillonite (Fe-OMT) and zinc borate (ZnB) presented perfect synergistic effect on GRPA6/MPP composites [7]. And also, Chen et al. synthesized a novel flame retarded TTPSi which contained silicon and caged bicyclic phosphate groups, and 25 wt% of TTPSi loading could result in satisfied flame

* Corresponding authors. Address: State Key Laboratory of Fire Science, University of Science and Technology of China, 96 Jinzhai Road, Hefei, Anhui 230026, PR China. Tel./fax: +86 551 3601664 (Y. Hu), tel.: +86 551 3600419 (X. Gong).
E-mail addresses: yuanhu@ustc.edu.cn (Y. Hu), gongxl@ustc.edu.cn (X. Gong).

1359-835X/$ - see front matter © 2013 The Authors. Published by Elsevier Ltd. All rights reserved.
http://dx.doi.org/10.1016/j.compositesa.2013.07.001

retardancy and smoke suppression of PA6/TTPSi composites [9]. Ke et al. synthesized a hyperbranched charring and foaming agent (HCFA) and combined it with APP to form a novel intumescent flame retardant system. They found that when the flame retardant loading was 25 wt%, the composites reached a high LOI value of 36.5 vol% with UL94 V0 rating [10].

Recently, metal hypophosphite was used as a novel flame retardant for glass-fiber reinforced polyamide composites and polyester composites [11–15]. Wang et al. prepared flame retarded glass-fiber reinforced polyamide 6 (FR-GRPA) composites based on aluminum hypophosphite (AHP) which could pass UL-94 V-0 rating with AHP loading of 20 wt% [11]. They also fabricated aluminum alkyl hypophosphite based flame retardant glass-fiber reinforced polyamide 6 (FR-GRPA) composites which only needed 15 wt% of flame retardant loading to reach perfect flame retardant properties [12]. Braun et al. also found that aluminum diethyl phosphinate presented perfect flame retardancy in fiber-reinforced poly(1,4-butylene terephthalate) (GRPBT) composites [14,15]. However, in most GRPBT or GRPA composites, the mechanical properties and thermal stability were affected by addition of the aluminum hypophosphite, which limited the use of AHP in the above composites.

Very recently, lanthanum hypophosphate (LaHP) was used as a novel flame retardant and presented excellent results in glass fiber reinforced polyester composites [16]. Yang et al. combined lanthanum hypophosphite with melamine cyanurate (MCA) to form a novel flame retardant system, which significantly reduced the flammability of GRPBT composites. Inspired by the above research, lanthanum hypophosphite (LaHP) was successfully synthesized and prepared flame retardant glass-fiber reinforced polyamide 6 composites (FR-GFPA). The combustion properties of the composites were measured by LOI, UL-94 and cone calorimeter test. The dynamic mechanical and tensile properties for these composites were also studied. Furthermore, the char residues were analyzed by SEM.

2. Experimental section

2.1. Materials

Lanthanum(III) chloride heptahydrate (analytical grade) were supplied by Ruibokang rare earth materials Co., Ltd. Sodium hypophosphite (analytical grade) and concentrated hydrochloride acid were supplied by Sinopharm Chemical Reagent Co., Ltd. Polyamide 6 resin (UBE 1013B) in granular form was supplied by UBE group (Thailand). The deionized water was used in this work.

2.2. Synthesis of rare earth hypophosphite

In typical experiment, 31.8 g (0.3 mol) sodium hypophosphite was dissolved in 200 ml deionized water, and the pH of the solution was regulated to 1.4 by 5 wt% hydrochloride acid solution and added into 1000 ml three-neck flask equipped with a mechanical stirrer. Afterwards, a solution with 37.1 g (0.1 mol) lanthanum chloride heptahydrate and 200 ml deionized water was added dropwise to the above flask at 50 °C under stirring in a nitrogen atmosphere for 4 h. The resulting solids was collected by suction filtration, washed with deionized water, and dried at 200 °C for 4 h to remove the water of crystallization [17].

2.3. Preparation of flame retardant FR-GFPA composites

Polyamide 6 resin, glass fiber and LaHP were dried at 80 °C overnight before used. All the samples were prepared by a two roll mixing mill (XK-160, Jiangsu, China) at 230 °C and the rotation speed of screw was 80 rpm. Polyamide 6 resin was firstly added to the mill at the beginning of the blending procedure. After polyamide 6 resin was molten, the additives were then added to the matrix and processed for 10 min until a visually good dispersion was achieved. The mixtures after mixing were cut into pellets and then hot-pressed into sheets under 10 MPa for 10 min. The sheets were cut into suitably sized specimens for fire testing. The detailed formulations of the samples are shown in Table 1.

2.4. Measurement and characterization

Fourier transformed infrared spectra spectroscopy (Nicolet 6700FT-IR spectrophotometer) was also used to characterize the residues using KBr disc. The transmission mode was used and the wave number range was set from 4000 cm^{-1} to 400 cm^{-1}. Thermal properties of LaHP, GFPA and GFPA/LaHP composites were performed on a TGA Q5000 IR (with accuracy and precision were ±0.1% and ±0.01%, respectively) thermal gravimetric analyzer (TA instruments) under both nitrogen and air atmosphere at a heating rate of 20 °C/min.

Limiting oxygen index (LOI) values of the composites were measured by Limiting Oxygen Index Analyzer (Jiangning Analysis Instrument Company, China) according to the ASTM standard D2863. The samples used for the test were of the dimension of $100 \times 6.5 \times 3.0\ mm^3$. Underwriters Laboratories 94 testing (UL-94) was carried out on a CFZ-2 type instrument (Jiangning Analysis Instrument Company, China) according to ASTM D3801. The specimens used for the test were of the dimensions of $130 \times 13 \times 3\ mm^3$. Cone calorimeter combustion tests were performed on the cone calorimeter (Fire Testing Technology, UK) according to ISO5660 standard procedures, each sample with dimension $100 \times 100 \times 3\ mm^3$ was wrapped in an aluminum foil and exposed horizontally to 35 kW/m^2 external heat flux.

Char residues of the samples after calorimeter test were further analyzed by scanning electron microscope AMRAY1000B with accelerating voltage of 20 kV. The specimens were sputter-coated with a conductive layer. Dynamic mechanical properties were measured with a DMAQ800 (TA, USA). The dynamic storage modulus was determined at a frequency of 10 Hz and a heating rate of 5 °C in the temperature range 25–200 °C. The mechanical properties were measured with a universal testing machine (WD-20D) according to ASTM D-638 at temperature 25 ± 2 °C. The specimens were prepared by cutting strips 4.0 ± 0.1 mm wide and 1.0 ± 0.05 mm thick. The crosshead speed was 20 mm/min. An average of at least five individual determinations was obtained. The dispersion of additives in GFPA and FR-GFPA composites was investigated by scanning electron microscope AMRAY1000B. The samples were cryogenically fractured in liquid nitrogen and then sputter-coated with a conductive layer. The accelerated voltage is 20 kV.

3. Results and discussion

3.1. Characterization of lanthanum hypophosphite

FTIR spectrum of lanthanum hypophosphite is shown in Fig. 1. The broad band between 3000 and 3500 cm^{-1} can be ascribed to

Table 1
Results of UL-94 and LOI tests for GFPA and FR-GFPA composites.

Sample	Composition (wt%)			LOI	UL-94. 3.2 mm bar		
	PA6	GF	LaHP		t_1/t_2[a] (s)	Dripping	Rating
GFPA	70	30	–	23.5	BC[b]	Y	NR[c]
GFPA/LaHP5	65	30	5	24.5	BC	Y	NR
GFPA/LaHP10	60	30	10	25	BC	Y	NR
GFPA/LaHP15	55	30	15	26	1.7/9.5	N	V1
GFPA/LaHP20	50	30	20	27.5	1.0/3.2	N	V0

[a] t_1 and t_2, average combustion times after the first and the second applications of the flame.
[b] BC, burns to clamp.
[c] NR, not rated.

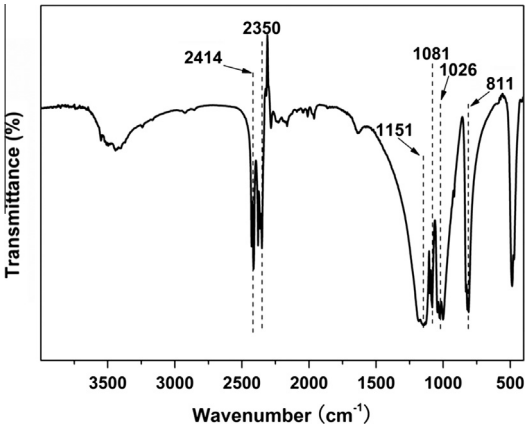

Fig. 1. FTIR spectra of LaHP.

asymmetrical and symmetrical stretching vibrations of O–H bond in the form of absorbed water in LaHP. The peaks at 2414 and 2350 cm^{-1} corresponds to PH_2 stretching [18]. The bands between 1026 and 1151 cm^{-1} are ascribed to bending modes of PH_2 [19]. The peak at 1081 cm^{-1} is attributed to P–O modes. The medium intensity peak at 811 cm^{-1} can be attributed to the rocking mode of PH_2.

The SEM micrographs of LaHP are presented in Fig. 2. The micrographs show rod-like crystals have uniform dimension. It presents a size of 20–80 μm in length and 5–20 μm in width. The magnified micrograph of Fig. 2b indicates that the surface shows folded structure which may result from the high temperature processing.

Thermogravimetric analysis is used to further investigate thermal stability of LaHP. The onset degradation temperature $T_{-5\%}$ is defined as the temperature at 5 wt% weight loss, and T_{max} is defined as the temperature at which the sample presents the maximal mass loss rate. TG and DTG curves of LaHP in nitrogen atmosphere are shown in Fig. 3a. LaHP presents the onset decomposition temperature at 350 °C, and the maximal mass loss rate occurs at 350 °C and 787 °C, indicating that LaHP shows similar degradation process to that of AHP [20]:

$$2La(H_2PO_2)_3 \xrightarrow{\Delta} La_2(HPO_4)_3 + 3PH_3 \quad (1)$$

$$2La_2(HPO_4)_3 \xrightarrow{\Delta} La_4(P_2O_7)_3 + 3H_2O \quad (2)$$

The first decomposition process attributes to the degradation of LaHP, which results in the formation of $La_2(HPO_4)_3$ and release of phosphine. The second decomposition process belongs to the further degradation of $La_2(HPO_4)_3$. Thermal behavior of LaHP is further investigated in air atmosphere and the corresponding curves are shown in Fig. 3b. It is interesting to find that LaHP presents a mass increase process at the temperature range from 336 to 354 °C with a T_{max} at 345 °C. It also shows another mass increase

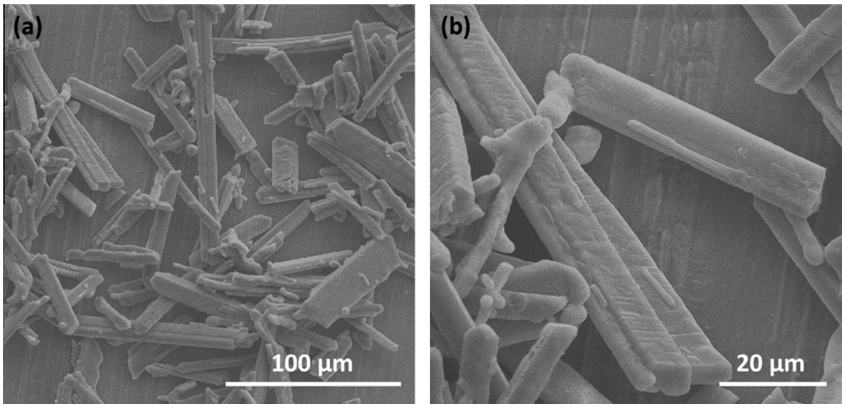

Fig. 2. SEM images of LaHP.

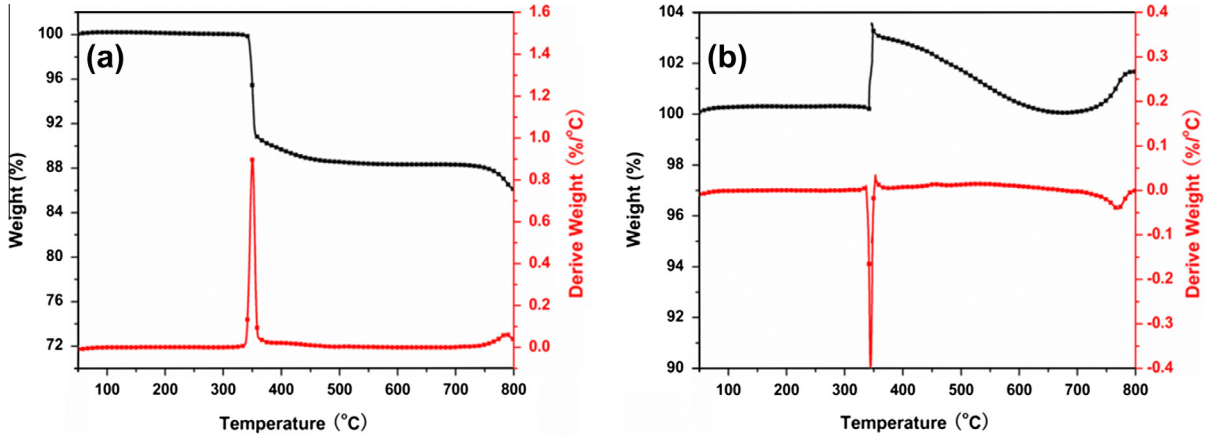

Fig. 3. TG and DTG curves of LaHP under nitrogen and air atmosphere: (a) nitrogen atmosphere; and (b) air atmosphere. (For interpretation of the references to color in this figure legend, the reader is referred to the web version of this article.)

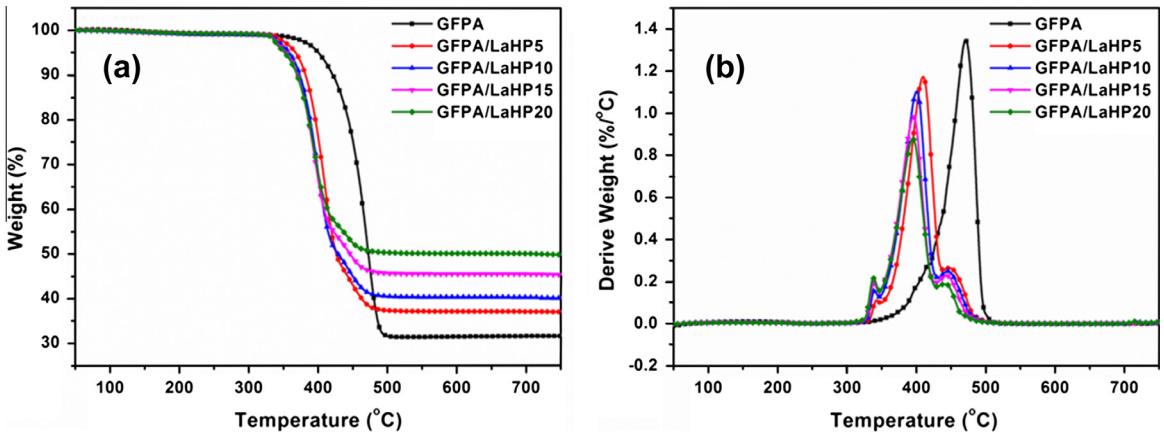

Fig. 4. TG and DTG curves of GFPA and FR-GFPA composites under nitrogen atmosphere. (For interpretation of the references to color in this figure legend, the reader is referred to the web version of this article.)

Table 2
TG and DTG data of LaHP, GFPA and FR-GFPA composites under nitrogen atmosphere.

Sample	$T_{-5\%}$ (°C)	T_{max1}[a] (°C)	T_{max2} (°C)	T_{max3} (°C)	Residues[b] (wt%)
LaHP	350	350	–	–	88.0
GFPA	401		–	471	31.6
GFPA/LaHP5	368	342	410	448	36.9
GFPA/LaHP10	358	339	400	445	49.9
GFPA/LaHP15	354	338	396	442	45.1
GFPA/LaHP20	352	338	395	437	49.5

[a] Maximal mass loss rate.
[b] At 800 °C.

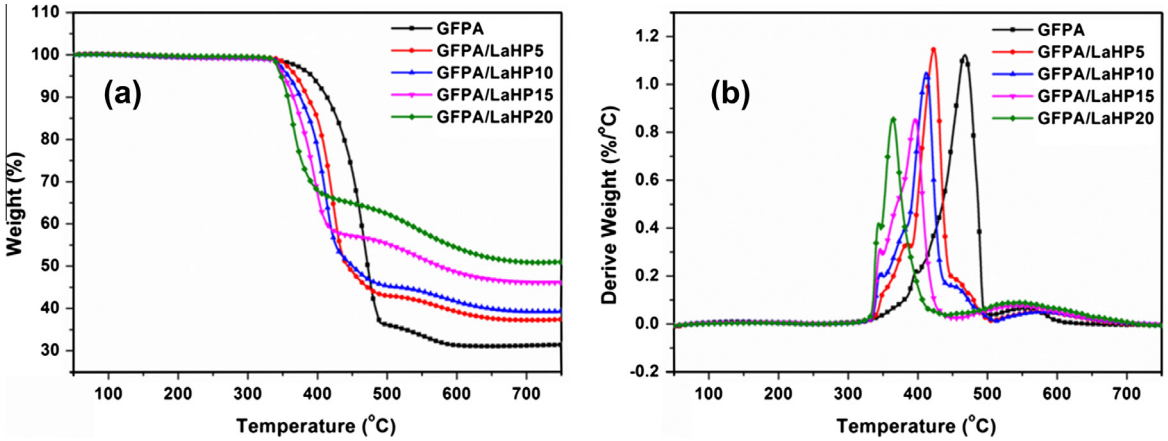

Fig. 5. TG and DTG curves of GFPA and FR-GFPA composites under air atmosphere. (For interpretation of the references to color in this figure legend, the reader is referred to the web version of this article.)

process at 739–790 °C with a T_{max} at 769 °C. The char residue of LaHP at 800 °C is 101.7 wt%, indicating some oxidation process occurs, which is similar to AHP [20]:

$$2La(H_2PO_2)_3 \xrightarrow{\triangle} La_2(HPO_4)_3 + 3PH_3 \quad (3)$$

$$PH_3 + 2O_2 \xrightarrow{\triangle} H_3PO_4 \quad (4)$$

$$2La_2(HPO_4)_3 \xrightarrow{\triangle} La_4(P_2O_7)_3 3H_2O \quad (5)$$

$$nH_3PO_4 \xrightarrow{\triangle} \left[\begin{array}{c} O \\ \| \\ P \\ | \\ OH \end{array}\right]_n + nH_2O \quad (6)$$

LaHP decomposes firstly with releasing phosphine, resulting in the formation of $La_2(HPO4)_3$. The phosphine is further oxidized by oxygen and generates phosphoric acid. When the temperature increases, phosphoric acid dehydrates and releases water, resulting

Table 3
TG and DTG data of LaHP, GFPA and FR-GFPA composites under air atmosphere.

Sample	$T_{-5\%}$ (°C)	T_{max1}[a] (°C)	T_{max2} (°C)	T_{max3} (°C)	Residues[b] (wt%)
LaHP	–	345	–	769	100.6
GFPA	392	397	467	553	31.7
GFPA/LaHP5	369	384	423	570	37.6
GFPA/LaHP10	358	346	412	583	39.5
GFPA/LaHP15	352	346	396	541	46.2
GFPA/LaHP20	348	344	386	542	51.2

[a] Maximal mass loss rate.
[b] At 800 °C.

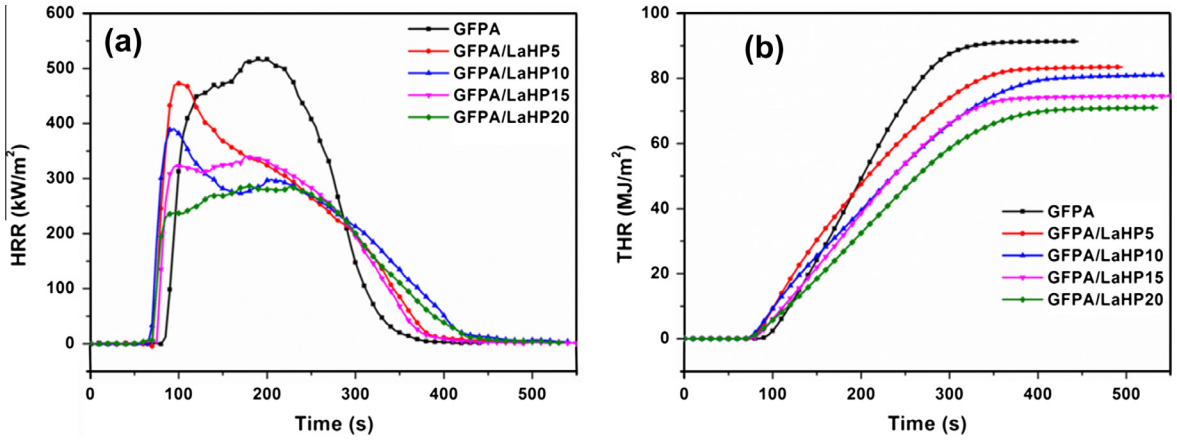

Fig. 6. HRR and THR curves of GFPA and FR-GFPA composites from cone calorimeter test. (For interpretation of the references to color in this figure legend, the reader is referred to the web version of this article.)

Table 4
Cone calorimeter data for GFPA and FR-GFPA composites at 35 kW/m^2. (TTI: time to ignition, ±2 s; PHRR: peak heat release rate, ±15 kW/m^2; T_p: time to pHRR, ±2 s; THR: total heat release, ±0.5 MJ/m).

Sample	TTI (s)	T_p (s)	pHRR (kW/m^2)	THR (MJ/m^2)	FPI (m^2 s/kW)	FIGPA (kW/m^2 s)
GFPA	71	190	517	91.3	0.14	2.72
GFPA/LaHP5	63	100	472	83.5	0.13	4.72
GFPA/LaHP10	60	95	390	81.0	0.15	4.10
GFPA/LaHP15	66	175	340	74.6	0.19	1.94
GFPA/LaHP20	62	180	286	71.0	0.22	1.59

Table 5
DMA data for GFPA and FR-GFPA composites.

Sample	$T_{tan\delta}$ (°C)	Storage modulus (GPa)		
		30 °C	90 °C	150 °C
GFPA	75.0	32.8	17.0	11.1
GFPA/LaHP5	80.0	61.7	33.6	21.9
GFPA/LaHP15	83.9	86.6	49.9	31.4
GFPA/LaHP20	82.4	64.2	38.4	25.1

in the formation of polyphosphoric acid which can promote the formation of char residue. At the second stage, $La_2(HPO_4)_3$ further degrades and forms $La_4(P_2O_7)_3$.

3.2. Thermal degradation behaviors

TG and DTG curves of GFPA and FR-GFPA composites in nitrogen atmosphere are shown in Fig. 4 and the corresponding data are listed in Table 2. GFPA presents onset decomposition temperature at 401 °C and T_{max} at 471 °C with char residue of 31.6 wt% at 800 °C.

All the FR-GFPA composites containing LaHP show three decomposition processes. The first stage shows T_{max} at 338–342 °C can be attributed to the decomposition of LaHP, the second stage presents T_{max} at the range of 395–410 °C corresponds to the degradation of polyamide matrix, the third one at 437–448 °C results from the further degradation of char residue. GFPA/LaHP5, GFPA/LaHP10, GFPA/LaHP15 and GFPA/LaHP20 show the decomposition temperature at 368, 358, 354 and 352 °C, respectively, which indicates that the addition of LaHP decreases the thermal stability of the composites at low temperature. However, the residues of these four composites are 36.9, 39.9, 45.1 and 49.5 wt%, respectively, indicating that LaHP significantly increases the thermal stability of the FR-GFPA composites at high temperature.

The decomposition behaviors of GFPA and FR-GFPA are further investigated by TGA in air atmosphere. The TG and DTG curves are presented in Fig. 5, and the corresponding data are listed in Table 3. GFPA shows the onset decomposition temperature at 392 °C, which is 9 °C lower than that in nitrogen atmosphere, indicating lower thermal stability of GFPA in air atmosphere. It presents three stages decomposition process at 397, 467 and 553 °C, which is more complicated compared with that in nitrogen atmosphere. For FR-GFPA composites containing LaHP, GFPA/LaHP5 shows the onset decomposition temperature at 369 °C, and the further addition of LaHP result in onset decomposition temperature at 358, 352 and 348 °C. This phenomenon comes from the less stability of LaHP. FR-GFPA composites all show three stages decomposition process which is similar to those in nitrogen atmosphere. However, it is interesting to find that the third decomposition process occurs at the broad range of 500–650 °C, showing much higher T_{max} value compared with those in nitrogen atmosphere. This phenomenon can be explained as follows: the third decomposition process

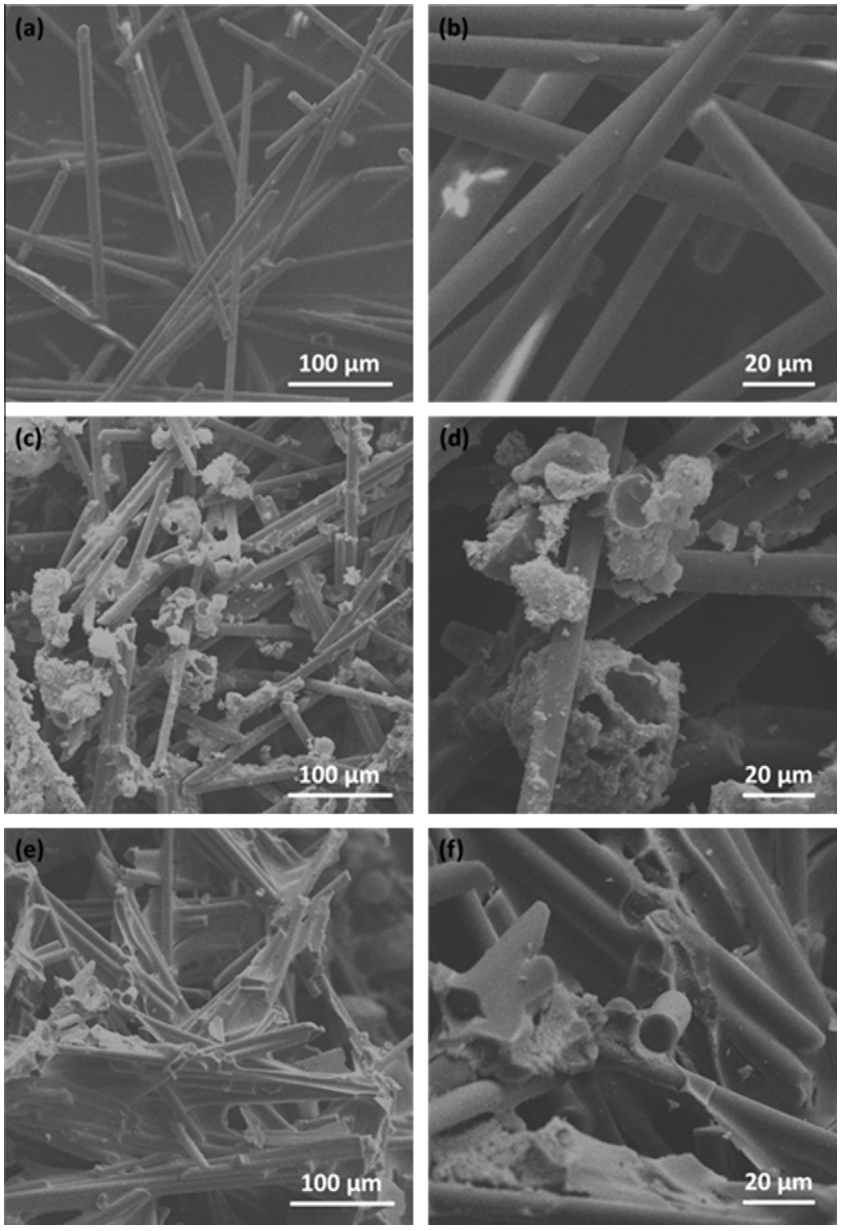

Fig. 7. SEM images of residues from GFPA and FR-GFPA composites after cone calorimeter tests: GFPA (a and b); GFPA/LaHP10 (c and d); GFPA/LaHP20 (e and f).

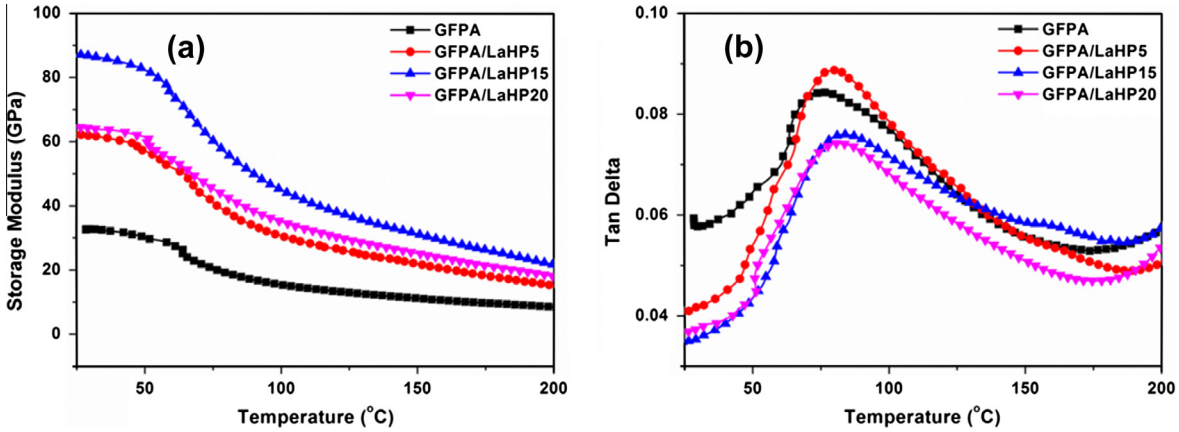

Fig. 8. Storage modulus and tan δ curves of GFPA and FR-GFPA composites from DMA testing. (For interpretation of the references to color in this figure legend, the reader is referred to the web version of this article.)

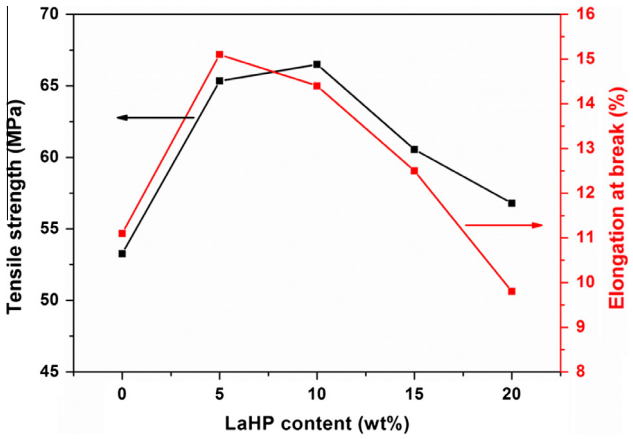

Fig. 9. Effect of LaHP loading on the mechanical properties of GFPA and FR-GFPA composites. (For interpretation of the references to color in this figure legend, the reader is referred to the web version of this article.)

contains two parts, the oxidation of unstable char and the oxidation of phosphine; the former results in loss while the later increases the weight. The char residues of FR-GFPA composites in air atmosphere are all higher than their counterpart in nitrogen atmosphere; this may come from the oxidation of phosphine to form polyphosphate which promotes the formation of stable char.

3.3. LOI and UL-94 rating

LOI and UL-94 tests are used to characterize the flame retardant behaviors of FR-GFPA composites, and the corresponding data are presented in Table 1. GFPA presents a LOI value of 23.5 vol% with no rating in UL-94 test. LOI value of GFPA/LaHP composites is increased from 24.5 vol% of GFPA/LaHP5 to 27.5 vol% of GFPA/LaHP20. GFPA/LaHP5 and GFPA/LaHP10 present no rating. The further increase of LaHP loading to 15 wt%, GFPA/LaHP15 shows V1 rating, and the dripping problem is inhibited. When 20 wt% of LaHP is added, GFPA/LaHP20 presents V0 rating and the total burning time is much shorter than that of GFPA/LaHP15.

3.4. Cone calorimeter testing

Cone calorimeter test based on oxygen consumption principle has been widely used to evaluate the combustion behaviors of materials since it is developed at NBS (now NIST) in 1982 [21]. Although it is a bench-scale test, some results of cone calorimeter tests show perfect correlation with real fire condition [22,23]. So, it is a useful method to predict the combustion performance of materials in real condition. HRR and THR curves of FGPA and FR-GFPA composites are shown in Fig. 6, and the corresponding data are shown in Table 4. As shown in Fig. 6a, GFPA composite presented gently pHRR value of 517 kW/m^2; for FR-GFPA composites, GFPA/LaHP5, GFPA/LaHP10, GFPA/LaHP15 show sharp pHRR values of 472, 390 and 340 kW/m^2, with a reduction of 8.7%, 24.6% and 34.2% compared with that of GFPA composite, respectively. When 20 wt% LaHP is added, the HRR curves become gently with a peak of 286 kW/m^2, with a further reduction of 44.7% compared with that of GFPA. Fig. 6b shows THR curves of GFPA and FR-GFPA composites. At the end of the burning, GFPA shows a THR value of 91.3 MJ/m^2. The addition of LaHP results in gradually decreased trend of THR value for FR-GFPA composites with the increase of LaHP loading. The time to ignition (TTI) of GFPA composite is 71 s, while the FR-GFPA composites all show shorter TTI values compared with that of GFPA. This is because the acid sources derived from the decomposition of LaHP promotes the degradation of molecular chains of polyamide 6, resulting in the TTI values forward. In order to further investigate the fire hazard of GFPA and FR-GFPA composites, the fire performance index (FPI) and fire growth index (FIGPA) were introduced. FPI is defined as proportion of TTI and the pHRR value. It is reported that there is a certain correlation between the value of FPI of material and the time to flashover. As shown in Table 5, FPI values of FGPA/LaHP5 and FGPA/LaHP10 change little, but the further addition of LaHP results in a significant increase of FPI value, indicating the high loading of LaHP can significantly decrease the fire hazard of FR-FGPA composites. FIGPA is defined as the proportion of pHRR and time to peak heat release rate (T_p), which reflects the spread speed of the fire. The larger FIGPA value is, the higher hazard of the material is. However, in GFPA/LaHP5 and GFPA/LaHP10, T_p shows a significant decrease, thus the FIGPA are significant increased, indicating the fire spread speed is significantly increased. However, the further addition of LaHP in GFPA/LaHP15 and GFPA/LaHP20 decreases the FIGPA value; this may result from the fact that the addition of LaHP is helpful to form compact layer which could delay the spread of fire. Apparently, the fire risk of GFPA/LaHP15 and GFPA/LaHP20 composite is much lower than that of GFPA.

In order to further investigate the flame retardancy, the char residues after cone calorimeter are analyzed by SEM. The char residue of GFPA composites shows almost glass fiber without any char in the two magnifications images (Fig. 7a and b). When 10 wt% LaHP is added, significant condensed products around glass fiber are improved in char residue of GFPA/LaHP10 (Fig. 7c and d). However, the char residue is quite coarse with many pores between the char residue and glass fiber. Undoubtedly, it was not effective for the porous char residue to insulate heat and mass transportation. The further increase of LaHP loading results in the formation of compact char residue, which can be observed in Fig. 7e and f. The glass fiber is almost covered with the condensed char without any pore. These results indicate that 20 wt% loading of LaHP can significantly increase the flame retardancy of FR-GFPA composites, which is consistent with LOI and UL-94 testing.

3.5. Dynamic mechanical properties

Dynamic mechanical analysis (DMA) is one of the most important techniques commonly used to measure the time, frequency, temperature dependency of the viscoelastic nature of polymers [24]. As shown in Fig. 8, the addition of LaHP results in a significant increase in storage modulus of FR-GFPA composites compared with GFPA. The trend of the storage modulus increases first and then decreased with the LaHP loading increases from 5 to 20 wt%. The corresponding data are shown in Table 5. As can be observed, GFPA/LaHP15 presents the highest storage modulus value of 86.6 GPa, which is 164% higher than that of GFPA (32.8 GPa) at 30 °C. The remarkable increase of storage modulus indicates that rod-like structure of LaHP particles function as reinforced agents in the whole temperature region. The temperature at maximum of tanδ ($T_{\tan\delta}$) is usually taken as glass transition temperature (T_g). As shown in Table 5, $T_{\tan\delta}$ values of FR-GFPA composites are 5.0–8.9 °C higher than that of GFPA. The increase in T_g values originates from that the rod-like LaHP particles limit the movement of polyamide 6 molecular chain.

3.6. Mechanical properties and dispersion analysis

Fig. 9 presents the tensile properties of GFPA and GFPA/LaHP composites with different LaHP loading. The tensile strength and elongation at break of FGPA composites are 52.3 MPa and 11.1%, respectively, which is consistent with the reported value [6]. The tensile strength is increased to 66.5 MPa of GFPA/10LaHP, with a 27% increase compared with GFPA. Although the further increase

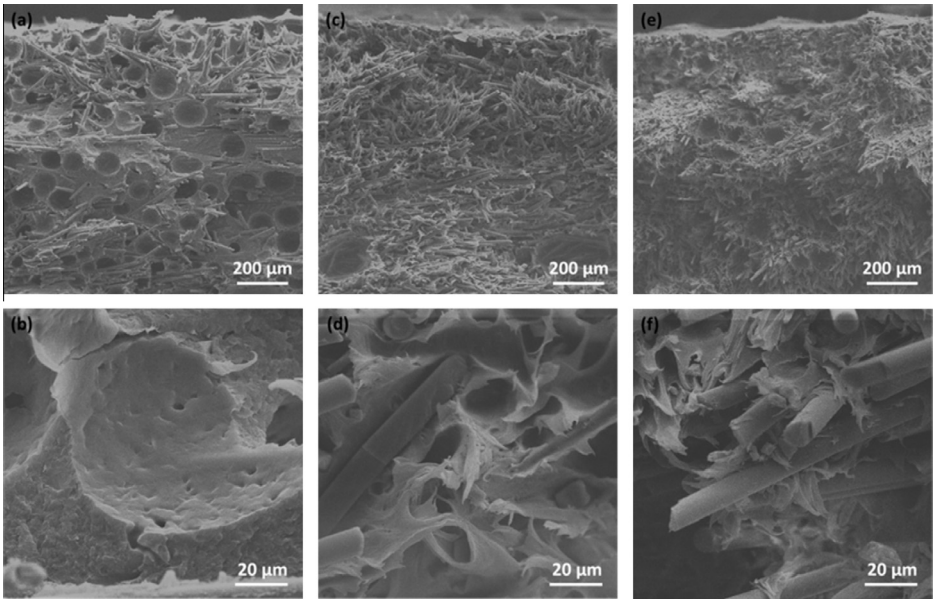

Fig. 10. SEM image of GFPA (a and b); GFPA/LaHP10 (c and d); GFPA/LaHP20 (e and f).

of LaHP loading results in a slight decrease in tensile strength, the values of GFPA/LaHP15 and GFPA/LaHP20 are both higher than that of GFPA. As shown in Fig. 9, the elongation at break of FR-GFPA composites except GFPA/LaHP20 show higher values compared with that of GFPA.

It can be obviously found that the tensile strength and elongation at break increase firstly and then decrease with the increase of LaHP loading, indicating the dispersion of LaHP and glass fiber play important role. So, scanning electron microscope (SEM) is used to further investigate the effect of particles (LaHP and glass fiber) dispersion on the mechanical properties, and the corresponding results are shown in Fig. 10. As shown in Fig. 10a, many bubbles are shown on the fractured surface of GFPA. And the high magnification of Fig. 10b shows that the fractured surface is smooth, the indicating bad compatibility between glass fibers and PA6 matrix. Fig. 10c and d presents the low and high magnification of GFPA/LaHP10, from which we can find that the LaHP and glass fiber are homogeneously dispersed in the matrix, and the fractured surface of GFPA/LaHP10 coarse, indicating good compatibility of the additives and PA 6 composites. As shown in Fig. 10e and f, when the LaHP loading increase to 20 wt%, glass fiber shows significant agglomeration of glass fiber in the fractured surface GFPA/LaHP20. The phenomenon is consistent with the DMA and mechanical property test, in the GFPA/LaHP composites with low LaHP loading, the LaHP can play as a reinforcement agent, increasing the tensile strength and storage modulus; however, the high LaHP loading decrease the matrix concentration, resulting in agglomeration of glass fiber which decrease the mechanical property and storage modulus of GFPA/LaHP composites.

4. Conclusion

In this work, lanthanum hypophosphite was synthesized by a facile method and used as a novel halogen-free flame retardant for glass fiber reinforced polyamide 6 composites. For FR-GFPA composites, the thermal stability in nitrogen and air atmosphere was investigated by TGA. The flame retardancy and combustion behaviors were characterized by LOI, UL-94 and cone calorimeter test. The mechanical properties were investigated by DMA, mechanical testing and SEM. TGA testing showed that the incorporation of LaHP decreased the thermal stability of FR-GFPA composites in low temperature but increased the char yields at high temperature. The FR-GFPA composite could pass V-0 rating with LOI value of 27.5 vol% when the LaHP loading was 20 wt%. Additionally, the results observed from cone calorimeter testing indicated that both of the pHRR and THR values were significantly reduced by the addition of LaHP. The char residues of GFPA/LaHP20 showed that the improvement of the flame retardancy was mainly attributed to the compact char as an effective barrier between polymer materials and flame during combustion. DMA and tensile testing results presented that both the modulus and tensile strength were increased first and then decreased with the increase of LaHP loading. The storage modulus of GFPA/LaHP15 was 164% higher than that of GFPA. The enhancement of mechanical properties resulted from reinforced effect of LaHP particles in the composites when the flame retardant loading was lower than 15 wt%. The high loading of LaHP gave rise to the decrease of mechanical properties due to the low matrix concentration and agglomeration of glass fiber. However, high LaHP loading was still needed to reach high flame retardancy for FR-FGPA composites, such as extinguishing in short time and no dripping.

Acknowledgements

This research was supported by National Basic Research Program of China (973 Program) (2012CB719701), the joint fund of Guangdong province and CAS (No. 2010A090100017), the Fundamental Research Funds for the Central Universities (WK2320000014) and The Opening Project of State Key Laboratory of Fire Science of USTC (HZ2010-KF06).

References

[1] Akkapeddi MK. Glass fiber reinforced polyamide-6 nanocomposites. Polym Compos 2000;21(4):576–85.
[2] Moriwaki T. Mechanical property enhancement of glass fibre-reinforced polyamide composite made by direct injection moulding process. Compos Part A 1996;27(5):379–84.
[3] Casu A, Camino G, Giorgi MD, Flath D, Laudi A, Morone V. Effect of glass fibers and fire retardant on the combustion behaviour of glass fibres-poly(butylene terephthalate) composites. Fire Mater 1998;22(1):7–14.
[4] Malchev PG, de Vos G, Picken SJ, Gotsis AD. Mechanical and fracture properties of ternary PE/PA6/GF composites. Compos Sci Technol 2010;70(5):734–42.

[5] Levchik SV, Camino G, Costa L. Mechanism of action of phosphorus-based flame retardants in nylon 6. I. Ammonium polyphosphate. Fire Mater 1995;19(1):1–10.
[6] Chen YH, Wang Q. Preparation, properties and characterizations of halogen-free nitrogen-phosphorous flame-retarded glass fiber reinforced polyamide 6 composite. Polym Degrad Stab 2006;91(9):2003–13.
[7] Tai QL, Yuen RKK, Yang W, Qiao ZH, Song L, Hu Y. Iron-montmorillonite and zinc borate as synergistic agents in flame-retardant glass fiber reinforced polyamide 6 composites in combination with melamine polyphosphate. Compos Part A 2012;43(3):415–22.
[8] Ricciardi MR, Antonucci V, Zarrelli M, Giordano M. Fire behavior and smoke emission of phosphate-based inorganic fire-retarded polyester resin. Fire Mater 2012;36(3):203–15.
[9] Chen J, Liu SM, Zhao JQ. Synthesis, application and flame retardancy mechanism of a novel flame retardant containing silicon and caged bicyclic phosphate for polyamide 6. Polym Degrad Stab 2011;96(8):1508–15.
[10] Ke CH, Li J, Fang KY, Zhu QL, Zhu J, Yan Q. Enhancement of a hyperbranched charring and foaming agent on flame retardancy of polyamide 6. Polym Adv Technol 2011;22(12):2237–43.
[11] Zhao B, Hu Z, Chen L, Liu Y, Liu Y, Wang YZ. A phosphorus-containing inorganic compound as an effective flame retardant for glass-fiber-reinforced polyamide 6. J Appl Polym Sci 2011;119(4):2379–85.
[12] Hu Z, Chen L, Lin GP, Luo Y, Wang YZ. Flame retardation of glass-fibre-reinforced polyamide 6 by a novel metal salt of alkylphosphinic acid. Polym Degrad Stab 2011;96(9):1538–45.
[13] Hu Z, Lin GP, Chen L, Wang YZ. Flame retardation of glass-fiber-reinforcedpolyamide 6 by combination of aluminum phenylphosphinate with melamine pyrophosphate. Polym Adv Technol 2011;22(7):1166–73.
[14] Braun U, Schartel B. Flame retardancy mechanisms of aluminium phosphinate in combination with melamine cyanurate in glass-fiber-reinforced poly(1,4-butylene terephthalate). Macromol Mater Eng 2008;293(3):206–17.
[15] Braun U, Bahr H, Sturm H, Schartel B. Flame retardancy mechanisms of metal phosphinates and metal phosphinates in combination with melamine cyanurate in glass-fiber reinforced poly(1,4-butyleneterephthalate): the influence of metal cation. Polym Adv Technol 2008;19(6):680–92.
[16] Yang W, Tang G, Song L, Hu Y, Yuen RKK. Effect of rare earth hypophosphite and melamine cyanurate on fire performance of glass-fiber reinforced poly(1,4-butylene terephthalate) composites. Thermochim Acta 2011;526(1–2):185–91.
[17] Seddon JA, Jackson ARW, Roman A, Kresiński RA, Platt AWG. Complexes of the lanthanide metals (La–Nd, Sm–Lu) with hypophosphite and phosphite ligands: crystal structures of $[Ce(H_2PO_2)_3(H_2O)]$, $[Dy(H_2PO_2)_3]$ and $[Pr(H_2PO_2)(HPO_3)(H_2O)]\,H_2O$. J Chem Soc Dalton Trans 1999;0:2189–96.
[18] Noisong P, Danvirutai C, Srithanratana T, Boonchom B. Synthesis characterization and non-isothermal decomposition kinetics of manganese hypophosphite monohydrate. Solid State Sci. 2008;10(11):1598–604.
[19] Yoshida Y, Inoue K, Kyritsakas N, Kurmoo M. Syntheses, structures and magnetic properties of zig-zag chains of transition metals. Inorg Chim Acta 2009;362(5):1428–34.
[20] Tang G, Wang X, Xing WY, Zhang P, Wang BB, Hong NN, et al. Thermal degradation and flame retardance of biobased polylactide composites based on aluminum hypophosphite. Ind Eng Chem Res 2012;51(37):12009–16.
[21] Barauskas V. Development of the cone calorimeter- a bench-scale heat release rate apparatus based on oxygen-consumption. Fire Mater 1984;8(2):81–95.
[22] Schartel B, Bartholmai M, Knoll U. Some comments on the use of cone calorimeter data. Polym Degrad Stab 2005;88(3):540–7.
[23] Laoutid F, Bonnaud L, Alexandre M, Lopez-Cuesta JM, Dubois Ph. New prospects in flame retardant polymer materials: from fundamental to nanocomposites. Mater Sci Eng 2009;63(3):100–25.
[24] Quan H, Zhang BQ, Zhao Q, Yuen RKK, Li RKY. Facile preparation and thermal degradation studies of graphite nanoplatelets (GNPs) filled thermoplastic polyurethane (TPU) nanocomposites. Compos Part A 2009;40(9):1506–13.